Received: 12 March 2021 | Revised: 22 April 2021 | Accepted: 7 May 2021

DOI: 10.1111/ppl.13457

ECOPHYSIOLOGY, STRESS AND ADAPTATION

Physiologia Plantarum

Freezing stress damage and growth viability in *Vaccinium macrocarpon* Ait. bud structures

Camilo Villouta | Beth Ann Workmaster | Amaya Atucha

Department of Horticulture, University of Wisconsin, Madison, WI, USA

Correspondence
Amaya Atucha, Department of Horticulture, University of Wisconsin, 1575 Linden Drive, Madison, WI 53706, USA.
Email: atucha@wisc.edu

Funding information
National Institute of Food and Agriculture, Grant/Award Number: 1009297

Edited by: M. Uemura

Abstract

After a freezing event, it can be challenging to extrapolate levels of freezing damage to plant growth viability based on the presence or absence of symptoms in specific bud tissues. This study investigated the relationship between freezing damage in terminal buds during ecodormancy and their viability during the subsequent growing season. We identified the bud structure that best explained this relationship, and developed a model to explain the changes in bud cold hardiness. Vertical shoots (uprights) of *Vaccinium macrocarpon* Ait. *were sampled in central Wisconsin during Spring of* 2018 and 2019. Sets of uprights with terminal buds were subjected to controlled freezing tests, followed by either visual freeze damage evaluation or assessment of shoot viability by growth assays. We determined the Browning Lethal-Temperature$_{50}$ (BLT_{50}), as temperature for 50% damage (tissue browning) at each bud structure, and Growth Lethal-Temperature$_{50}$ (GLT_{50}) temperature where 50% reduction in growth viability occurred. Two models were constructed to explain: (1) bud structure damage and growth viability, and (2) GLT_{50}'s seasonal changes, representing the cold hardiness variations, and environmental factors. The correlation between the BLT_{50} and GLT_{50} values was closest for the bud scales and bud axis, indicating the better correspondence between levels of freezing damage with the impact on the growth potential. In addition, the latter was also the most suitable candidate for modeling due to easier damage evaluation. The freezing stress damage of the bud axis explained comparatively best the resulting growth viability. Seasonal changes in GLT_{50} were best explained by temperature indices based on daily minimum and on maximum temperatures over 10-day periods. However, among the model components, daily maximum temperatures had the greatest influence on *V. macrocarpon* cold hardiness changes during ecodormancy.

1 | INTRODUCTION

Freezing temperatures are one of the most important factors defining the geographic distributions of woody plants (George et al., 1974; Parker, 1963). The growth limitations imposed by freezing events are augmented by increases in the durations and frequencies of extreme weather events that have been identified as consequences of climate change (Vasseur et al., 2014; Williams et al., 2015). Specifically, early fall or late spring freezing events have the potential to affect the spring phenology of plants through bud injury, resulting in damage to

developing organs (Augspurger, 2013; Inouye, 2000). To best understand the consequences of these injuries, it is necessary to improve our techniques and approaches to accurately evaluate and quantify injury symptoms to extrapolate them to growth impairment (Ritchie, 1991).

After a freezing event, the evaluation of injury symptoms in buds of woody species has mostly relied on visual observations and/or electrolyte leakage measurements (Stergios & Howell, 1973). In fruit crops and conifers, evaluation of freeze injury symptoms for damage estimation is typically performed by bud dissection and the quantification of the proportion of tissue darkening or water-soaked appearance (Burr et al., 1990; DeMoranville & Demoranville, 1997; Larsen, 2009; Moyer et al., 2011; Olszewski et al., 2017), changes due to the oxidation of polyphenols (Sakai & Larcher, 1987) and in the refractive index after cell membrane injury resulting in the leaking of cell contents (Gordon-Kamm & Steponkus, 1984; Steponkus, 1984; Takahashi et al., 2018; Webb et al., 1994). However, damage prediction based on visual symptoms is problematic, as often the presence or absence of symptoms does not always accurately reflect tissue viability. For example, freeze injuries may not result in visual symptoms, but may still result in damage, or vice versa (Ritchie, 1991). In the case of electrolyte leakage, the proportion of ion leakage often does not correlate directly with the proportion of cell death, making estimation of damage by this method inaccurate (Palta et al., 1977a, 1977b).

To accurately estimate damage based on the evaluation of visual symptoms, a predictable relationship between the extent and intensity of the symptoms and the range of growth impairment or yield loss needs to be established (Luoranen et al., 2004; Odlum & Blake, 1996; Stergios & Howell, 1973). Despite their limitations, visual evaluations can be used to determine the hardiness of plant tissues when these observations are paired with empirical evaluations of growth capacity and viability (Luoranen et al., 2004; Stergios & Howell, 1973). The concept of the frost or freeze killing point (Levitt, 1980) is defined as the lethal temperature (LT) at which an arbitrary percentage of the evaluated samples are killed. "LT_{50}" is the most common killing temperature designation used to represent a degree of cold hardiness. The identification of specific organs or tissues whose chronic damage correlates most closely to subsequent plant growth impairment would be instrumental to establish an accurate relationship between visual symptoms and the LT_{50} estimates.

Linking visual evaluation damage levels to subsequent plant growth viability is critical to establish temperature thresholds for plant protection and management. Fruit tree growers could use this information to determine freeze/frost protection management strategies or to assess pruning and crop load decisions post-freeze events (Larsen, 2009). Similarly, the tree industry could assess seedling and stock acclimation, ensuring their successful establishment (Glerum, 1985; Warrington & Rook, 1980). In addition, breeding programs could more effectively select and evaluate new cultivars for improved freezing stress resistance (Rodrigo, 2000; Salazar-Gutiérrez et al., 2016).

Vaccinium macrocarpon Ait., the American cranberry, is a woody perennial evergreen vine of commercial importance. In this agricultural production system, vines are typically established in sunken beds in lowland areas highly susceptible to freezing damage in spring. As a consequence, freeze protection of *V. macrocarpon* vines is the most time- and resource-consuming management practice for growers. Understanding the relationship between bud tissue freezing damage and subsequent growth viability for this fruit crop is critical for the determination of meaningful temperature thresholds that will result in more effective freeze protection strategies. This approach would be applicable to other woody plant species, as well.

The main objective of this study was to investigate the relationship between visual freeze damage in buds and subsequent growth viability, and to determine the bud structure that best explains this relationship. The second objective was to evaluate how the key environmental parameters of temperature and photoperiod contribute to changes in cold hardiness of dormant buds during ecodormancy in *V. macrocarpon*. To address these objectives, we evaluated the severity of freeze damage in five bud structures: bud scales, shoot apical meristem (SAM), bud axis, flower primordia, and stem section, and we paired these data with assessments of plant viability. Two models were constructed to explain the relationships between: (1) bud structure damage and growth viability and (2) seasonal cold hardiness changes and the environmental factors of temperature and photoperiod.

2 | MATERIALS AND METHODS

2.1 | Plant material

"HyRed" uprights of *V. macrocarpon* were collected from a single production bed at a commercial farm located in Nekoosa, WI (44°16′46.9″N, 89°55′00.4″W) in early spring in 2018 and 2019. Sampling occurred weekly or biweekly, starting when the ice covering the production bed had melted by at least 50% and continuing until buds reached the phenological stage of bud swell. This resulted in six sampling dates in 2018 (March 19, April 2, April 10, April 24, May 1, May 8) and five in 2019 (April 1, April 19, April 25, May 2, May 9). Plant material was obtained from three sections of the bed (dimensions of 245 × 50 m), resulting in the collection of approximately 400 vertical shoots (uprights) per sampling area. Uprights were transported in zippered plastic bags in coolers with ice. Once in the laboratory, samples were sorted and processed immediately. Uprights with a reproductive medium size of 1–2 mm diameter, a tight ecodormant bud and a stem length no shorter than 10 cm were selected for controlled freezing tests (CFTs) and growth viability evaluation.

2.2 | Environmental conditions

For both years, canopy-level air temperature was recorded at hourly intervals from January 1 until May 31 with shielded Hobo pendant data loggers (Onset Computer).

2.3 | Controlled freezing tests

CFTs were performed following the methodology described by Villouta et al. (2020) in a Tenney Model T2C programmable freezing chamber (Thermal Product Solutions). To monitor sample location temperature within the freezing chamber, two 50 ml capped plastic tubes, each containing a copper-constantan (Type T) thermocouple (22 AWG) were placed at different locations inside the freezer and connected to a Keithley 2700-DAQ-40 multimeter data acquisition system (Keithley Instruments). Temperature data were recorded through a Keithley add-in in Excel (Microsoft Corp.) at a 6-s interval.

Selected uprights were rinsed in tap water, cut underwater to 8 cm length and blotted dry with paper towels. Groups of five uprights were wrapped at their bases with a moist paper towel and placed in 50 ml plastic centrifuge tubes with plastic caps. Six replicate tubes were used for each evaluated temperature. A separate group of six replicates was kept on ice as an unfrozen control. For each CFT run, the freezing chamber temperature was set at 1°C for thermal equilibration, after which a ramping to −1°C followed at a rate of 1°C hr^{-1}. After holding for 30 min, trays were firmly tapped to stimulate ice nucleation and kept at −1°C for 1 h. Subsequently, three different freezing rates were used: 1, 2, and 4°C h^{-1}, where each rate was used between 0 and −6°C, −6 to −12°C, and from −12°C to the lowest evaluated temperatures at the respective CFT, respectively.

In both years, sets of tubes were evaluated at nine different temperatures, in 2018 ranging from 0 to −46°C for the first four sampling dates and from 0 to −26°C for the last two dates. For 2019, a temperature range from 0 to −50°C was used for the first two sampling dates and from 0 to −30°C for the last three sampling dates. Once each set of tubes was removed from the freezing chamber, they were placed in a cooler with ice for 12 h, then transferred to a refrigerator set at 4°C and kept in the dark for 3 days to allow injury recovery. Afterward, tubes were maintained at room temperature for 24 h in low light conditions to allow the expression of damage symptoms from the freezing exposure. Following this, samples were divided in two subgroups; one subgroup was prepared for terminal bud dissection for damage evaluation, while the second subgroup was placed in favorable growth conditions for regrowth evaluation.

2.4 | Bud damage evaluation

One subgroup of samples containing 15 buds per temperature treatment for each CFT performed was dissected to observe freezing damage according to the procedure described by Villouta et al. (2020). Evaluations were performed using an Olympus SZX12 dissection microscope with a 1X objective (Olympus Optical Company) and an attached Canon EOS Rebel T6i digital camera (Canon U.S.A., Inc.). For evaluation, leaves were removed from the uprights, and buds were excised from the stem, leaving approximately 5 mm of stem section attached. The bud and attached stem portion were cut longitudinally, with a double-edged razor blade for immediate damage evaluation. The following bud structures were evaluated for freezing damage severity: bud axis, bud scales, attached stem, SAM, and flower primordia (Figure 1). Severity of damage was assessed by the proportion of oxidative browning (Larsen, 2009) and water soaking appearance incurred by each structure, as described by Villouta et al. (2020). Damage was scored on a scale from 0 to 3, with 0 representing no damage and 3 representing complete damage in the structure.

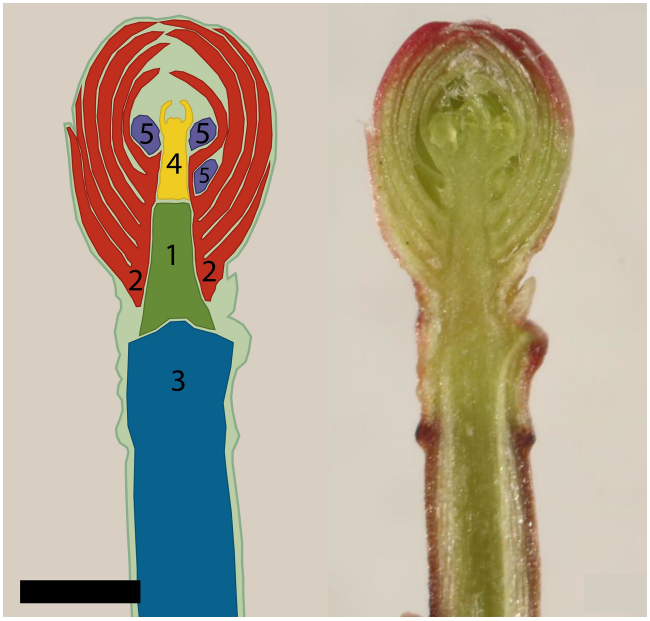

FIGURE 1 Longitudinal section of *Vaccinium macrocarpon* terminal bud depicting the five structures evaluated for freezing damage. Right: Longitudinal section of fresh sample. Left: Structures evaluated for freezing damage: 1 = bud axis; 2 = bud scales; 3 = stem section; 4 = shoot apical meristem; 5 = flower primordia. Scale equals 1 mm

2.5 | Growth evaluation

The second subgroup of samples containing 15 uprights per temperature treatment for each CFT performed was placed in favorable growth conditions to evaluate growth viability. Uprights were removed from the 50 ml plastic capped tubes and 1 cm of the bottom portion of the stem was removed. Groups of three uprights were placed in 70 ml glass tubes, for a total of five tubes per temperature treatment. Each glass tube of uprights received 5 ml of tap water, which was replaced weekly. Racks with glass tubes were placed under a long day regime of 16 h, provided by LED fixtures (Model: HY-MD-D169-S, Roleandro) containing blue and red lights of 460–465 nm and 620–740 nm, respectively, for a maximum PAR intensity of 150 μmol photons m^{-2} s^{-1}. The temperature of the growth environment ranged between 21°C and 24°C and was monitored with a Hobo pendant data logger (Onset Computer, Bourne). Visual weekly evaluations were performed to assess the phenological stage attained, as described by Workmaster et al. (1997), with stages assigned numbers from 0 to 8, with 0 being a tight bud and 8 showing blooming.

2.6 | Regression curve construction

The Gompertz function was fitted to the bud damage and growth viability data:

$$Y = a\exp[-\exp(b - kX)]$$

where *a*, *b* and *k* are parameters to be determined. Bud damage data were organized by averaging scores by structure of the 15 evaluated buds for each CFT temperature, and then plotting these against temperature for each sampling date. For each evaluated structure at each sampling date, the Gompertz function was fitted to the damage scoring. This method was based on Workmaster and Palta (2006), adapted from Lim et al. (1998). To define the best fit, the Gauss-Newton method was used through the NLIN procedure in the statistical software SAS (SAS Institute). From the resulting curves for each sampling date and bud structure, the temperature at which 50% (level 1.5) damage occurred was estimated from the fitted curves and designated as the Browning LT_{50} (BLT_{50}).

For the growth viability data, the Gompertz function was fitted following the same procedure as for bud damage data. For each sampling date, the fitting process used the phenology evaluations after six weeks of exposure to favorable growing conditions. Due to the Gompertz function requirement of a lower asymptote of zero, the phenology scale of 0 for "tight bud" and 8 for "bloom" was used. The temperature at which growth viability was compromised to 50% of the undamaged controls (represented by the upper asymptotes of the fitted curves) was calculated as an indicator of cold hardiness and designated as the Growth LT_{50}, or GLT_{50} (Figure 2). The temperature at which the greatest rate of growth impairment occurred was calculated as the peak value of the first derivative of the fitted Gompertz curves (Figure 2) and was designated as T_{max}.

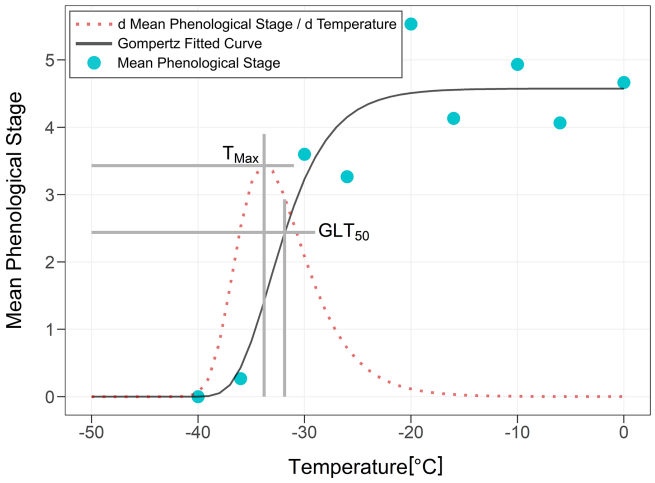

FIGURE 2 Example of curve-fitting and determination of *Vaccinium macrocarpon* bud cold hardiness estimates using the Gompertz function, based on the growth viability of terminal buds exposed to sequential freezing temperatures. Each point represents the mean phenological stage ($n = 15$) reached after sample exposure to favorable growth conditions for six weeks. The GLT_{50} represents the temperature of 50% growth viability. T_{max} represents the temperature of maximal rate of growth viability loss, identified by the first derivative of the fitted curve (dotted curve)

Average BLT_{50}, GLT_{50}, and T_{max} values, as well as standard errors, were obtained by a bootstrapping method based on Workmaster and Palta (2006), in which sampling with replacement strategy was applied to the original set of values. This process was repeated 1000 times for each sampling date, and from each new dataset generated, a set of Gompertz parameters was calculated. From the subsequent new sets of BLT_{50}, GLT_{50}, and T_{max} values, means and standard errors were calculated.

2.7 | Bud damage model (BD model)

To study the correlation between bud structure freeze damage severity and subsequent bud growth viability, a statistical model named "Bud Damage model" (BD model) was developed. A new data set was created that included one new variable, the percentage of growth viability, which was estimated from the fitted curves. One hundred percent growth viability was taken as the maximum value of the upper asymptote, as determined by the *a* parameter from the Gompertz equation. Zero percentage growth viability was taken as the lower asymptote, which was the phenological stage of 0 (tight bud). The other variable of the new data set was the average damage severity incurred by a bud structure at the CFT temperatures for each sampling date. Pearson's correlation coefficients calculated for this data set, plus consideration of the practical ease and reliability of symptom evaluation, were the criteria applied for selection of the bud structure whose damage expression best indicated subsequent growth capacity.

Following the bud structure selection, the BD model was constructed using a logistic regression with a quasibinomial distribution in R (ver. 3.5.1, R Foundation for Statistical Computing). The damage scores for the selected structure at each date and tested temperature were used as the explanatory variable, with the corresponding percentage of growth viability estimated from the fitted curves as the response variable. From this preliminary model, outliers were identified as those data points with standardized residuals greater or less than three standard deviations above or below zero and were removed. From this refined dataset a final model was fitted, followed by final testing with the Hosmer-Lemeshow goodness-of-fit test for logistic regression.

2.8 | Cold hardiness model (CH model)

Stepwise linear regression and normal distribution were used to develop a second model, named the "Cold Hardiness model" (CH model), to explain GLT_{50} changes in relation to climatic components. The explanatory variables tested for the combined set of 11 sampling dates were Julian day, photoperiod, hourly temperature, daily maximum temperature, daily minimum temperature, accumulated growing degree days with base temperature (T_{base}) values

ranging from 0 to 5°C, and a temperature index (σ_T) calculated for 7 (σ_{T7}), 10 (σ_{T10}), 12 (σ_{T12}), and 14 (σ_{T14}) preceding days, using either hourly, daily maximum, or daily minimum temperatures. Growing degree days were calculated (start date of January 1st each year) by the method of DeMoranville et al. (1996), using the daily average derived from the daily maximum and daily minimum temperatures with a maximum limit of 29.4°C. σ_T was calculated using the following equations, as described by Londo and Kovaleski (2017):

$$T_E = \text{Temperature (hourly or daily)}$$

$$\sigma_T^2 = \sum_{i=1}^{n} (T_E \times |T_E|)_i$$

$$\sigma_T = sgn(\sigma_T^2) \times \sqrt{|\sigma_T^2|}$$

where T_E was modified to be either the hourly, daily maximum, or daily minimum temperature experience of the plant for a determined range of preceding "n" hours or days. In the cases of hourly temperature, the "n" values used were 168, 240, 288, and 336 h. In the cases of daily maximum or daily minimum temperatures, the equivalent "n" values used were 7, 10, 12, and 14 days. Extreme temperatures are influential in the calculation of σ_T in two contrasting ways. On the one hand, because T_E is squared, extreme temperatures exert significant influence in each calculated time period. In contrast, since σ_T considers the temperature experience for a set bracket of preceding days whose reference point continually shifts, the influences of infrequent and extreme temperatures are smoothed, resulting in a stabilizing effect.

Since R was not capable of running all 23 variables simultaneously in the backward stepwise regression procedure to determine the best full model, a matrix of the 48 possible full models was constructed. Each model included: (1) Julian day, (2) photoperiod, (3) hourly, daily maximum, or daily minimum temperature, (4) one of the six growing degree day calculations with base temperature from 0°C to 5°C and (5), one of the temperature indices (σ_{T7}, σ_{T10}, σ_{T12}, and σ_{T14}; calculated with either hourly, daily maximum, or daily minimum temperatures). Each model was subjected to a stepwise selection and multicollinearity evaluation through the variable inflation factor. The five models with the highest adjusted-R^2 values were further evaluated with diagnostic plots for the selection of the final CH model, determined by dominance analysis.

3 | RESULTS

3.1 | Environmental conditions

For the 2 years of this study, canopy level temperatures remained below or at 0°C from January until the second half of March, while the ice cover remained over the vines. Canopy level temperatures began rising around March 30, 2018 and March 21, 2019, as the ice cover melted, gradually exposing the vine canopy (Figure 3). The daily maximum average temperature in May each year was markedly different: 23.8°C and 18.5°C for 2018 and 2019, respectively. Our period of interest for *V. macrocarpon* bud sampling in Wisconsin is relatively short, occurring between the melting of the winter ice cover on buds to just before bud swell. In 2018, this sampling "window" occurred between March 19 and May 8, and in 2019 it was between March 23 and May 9. As a result, growing degree days started to accumulate by April 24 in 2018, in contrast to April 1, in 2019 (Table 1).

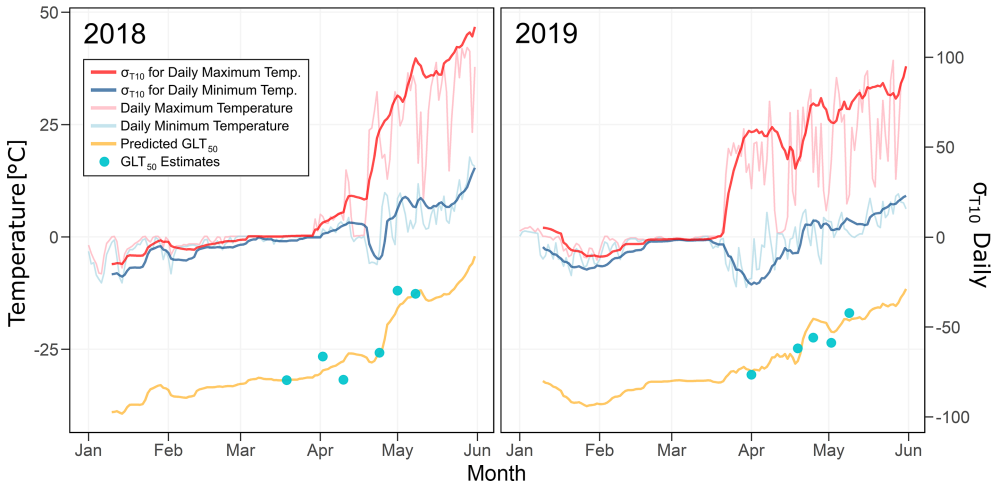

FIGURE 3 Daily minimum and maximum canopy-level temperatures, σ_{T10} for daily maximum and σ_{T10} for daily minimum temperatures, and estimated and predicted GLT_{50} values. Temperatures were measured at canopy height in a commercial *Vaccinium macrocarpon* farm in Nekoosa, WI from January 1 to June 30 of 2018 and 2019, respectively. The temperature indices σ_{T10} for daily maximum and σ_{T10} for daily minimum temperatures are calculated by multiplying each daily minimum or maximum temperature by its absolute value, then summing them for the preceding 10 days, and following by calculating the square root of the sum maintaining the original sign. The GLT_{50} estimates represent the temperature of 50% growth viability, as determined from the Gompertz function fitted to CFT data. The predicted GLT_{50} values were calculated using the cold hardiness model

TABLE 1 Growth degree days (GDD) accumulation according to sampling date

2018		2019	
Sampling date	**GDD**	**Sampling date**	**GDD**
19-Mar	0.0		
2-Apr	0.0	1-Apr	11.5
10-Apr	0.0	19-Apr	60.4
24-Apr	32.9	25-Apr	109.5
1-May	93.1	2-May	130.6
8-May	173.1	9-May	182.0

Note: GDD was calculated with base temperature 5°C for temperature recorded at canopy height. Temperature was measured from a commercial cranberry farm, located in Nekoosa, WI.

3.2 | Bud damage evaluation

Freezing damage assessment consisted of evaluating the extent of browning and water soaking in each of the five bud structures: bud axis, bud scales, flower primordia, SAM, and stem section. Gompertz regression curves were fitted to the data for each evaluated structure and sample date (Figure 4). All curves had an asymmetrical sigmoidal response, where the lower asymptote was close to zero, given that low levels of damage were observed in some buds at these warmer temperatures. "Early Spring" and "Late Spring" were defined as the periods before and after May 1, 2018 and April 25, 2019, which represent the shift in damage susceptibility to warmer temperatures (Figure 4). In general, Early Spring curves had a pattern of gradual increase in the levels of bud structure damage across the test temperatures. For these sampling dates, the levels of damage began to rise between −10°C and −20°C, reaching maximum levels of damage between −38°C and −50°C (Figure 4). During the late spring period, damage levels increased over a narrower temperature range, with the onset typically at relatively warmer temperatures than in Early Spring. In 2018, the increase in damage levels occurred from −6°C to −20°C in all bud structures, except the stem section, while in 2019, this range was more extended, from −6°C to −26°C.

The rate of damage increase in relation to temperature decrement varied by bud structure across the sampling period (Figure 4). During the first two sampling dates in 2018, the range from no damage to the maximal level of damage spanned from −15°C to −50°C (Figure 4). However, by mid to late April, the stem section and SAM had faster rates of injury increase, where the change from no damage to the maximal level of damage ranged between −25°C to −45°C, approximately double the rate observed in early spring (Figure 4). By May, all structures began exhibiting damage at warmer temperatures than in previous sampling dates, with the fastest increase from no damage to maximal damage in most structures spanning from −5°C to −30°C (Figure 4). During May 2019, the rapid increase in the rate of damage development was not as noticeable as in 2018 (Figure 4). However, the damage curves had a similar pattern when comparing the same sampling dates between years (Figure 4).

In 2018, flower primordia, stem section, and SAM had minimum BLT_{50} values of −37.1°C, −37.2°C, and −40.8°C, respectively. In comparison, bud axis and bud scales had minimum BLT_{50} values of −34.8°C and −35.1°C, respectively. In 2019, the differences in minimum BLT_{50} values between these two groups were not as large: −31.5°C, −32.3°C, and −33.7°C, for flower primordia, stem section, and SAM, respectively, and −32.1°C and −36.5°C for bud axis and bud scales, respectively.

3.3 | Growth evaluation

The resulting Gompertz fitted curve regressions for the growth evaluation data all had a sigmoidal shape. Across all the evaluated dates, there were ranges of relatively warmer freezing temperatures across which growth viability was not affected. Buds exposed to these "non-damaging" freezing temperature ranges achieved similar phenological stages as those in the unfrozen control and comprise the plateau portion of the upper asymptote of the regression curves (Figure 4). Reduction in growth viability shifted to warmer temperatures as the season progressed. For each sampling date, the range of temperatures in which growth viability was affected, by shifting from no impairment to maximum impairment got reduced and over time these ranges shifted to warmer temperature intervals, from −30°C to −20°C in "Early Spring" to −20°C to −8°C in "Late Spring."

GLT_{50} temperatures increased as the season progressed in both years (Figure 3). In Early Spring 2018, GLT_{50} temperatures did not change significantly, remaining below −25°C. However, by Late Spring that year, GLT_{50} values increased to −12°C (Table 2). In 2019, GLT_{50} values increased gradually over the sampling dates, ranging from −30°C to −17°C from Early Spring to Late Spring. Across sampling dates, GLT_{50} values corresponded with average relative bud structure damage levels between 0.2 and 1.0 for the stem section and SAM and 1.5 to 1.7 for the bud axis and bud scales (Table 3).

T_{max}, the temperature at which the maximal rate of growth viability reduction occurred, was generally at lower temperatures than the corresponding GLT_{50} (Figure 5). On average, the differences between T_{max} and GLT_{50} were larger in Early Spring than in Late Spring by 1.5°C and 0.5°C, respectively. This difference reflects the asymmetric nature of the regression curves, where the inflection point of the sigmoidal curves does not match the point of 50% of growth impairment, as represented by the GLT_{50}.

3.4 | Bud damage model (BD model)

The Pearson's correlation coefficients between relative freezing damage and percent growth viability were −0.89 for bud scales and flower primordia, −0.87 for stem section and SAM, and −0.92 for the bud axis, the highest correlation among the five structures. The purpose of the BD model was to explain the relationship between the levels of bud damage and the percentage of growth viability. The resulting model consisted of a

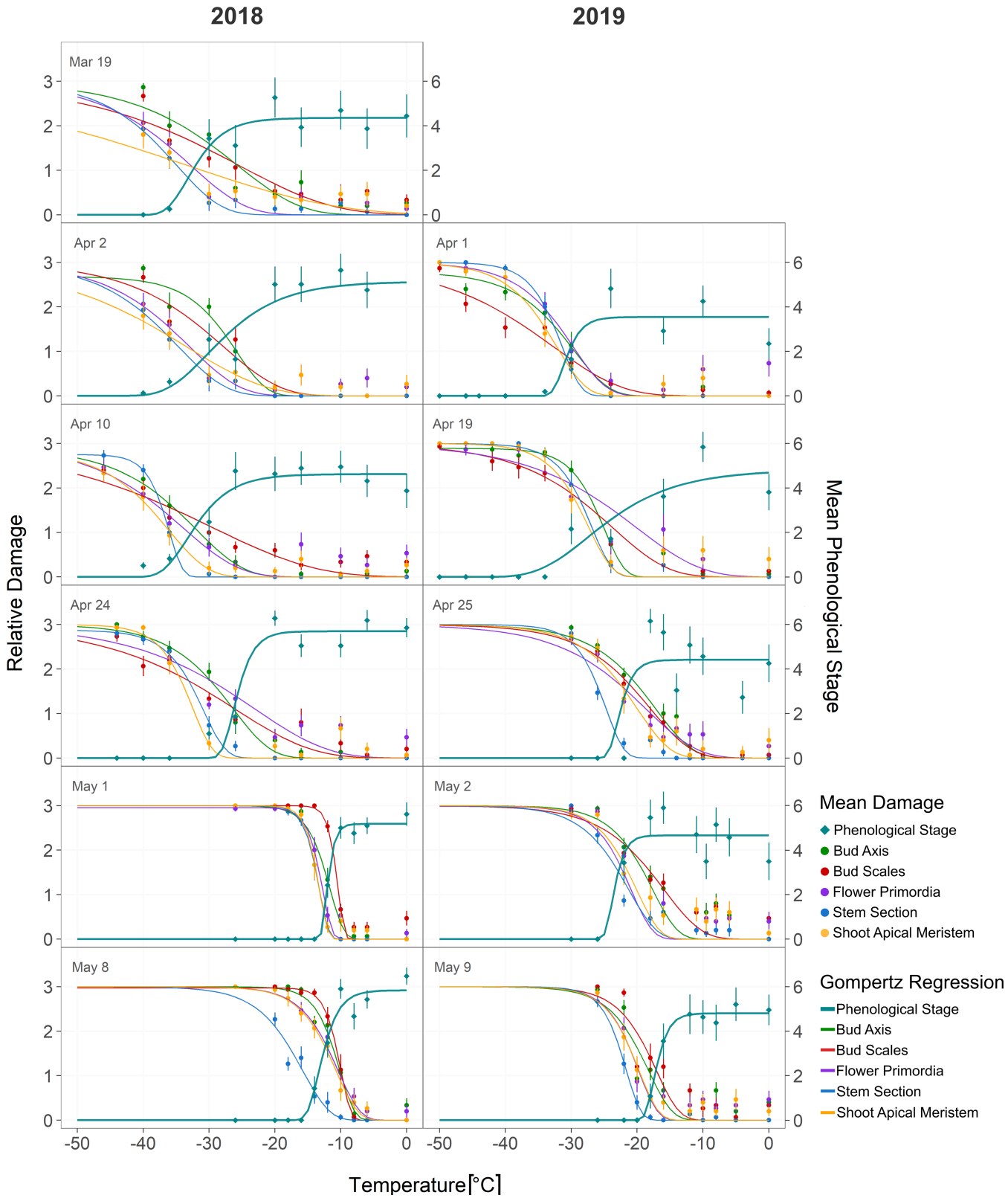

FIGURE 4 *Vaccinium macrocarpon* freeze damage scoring by bud structure and six-week growth viability evaluation after controlled freezing tests. Freeze damage symptoms were rated on a scale from 0 (no damage) to 3 (maximum damage). Growth viability evaluations are based on phenological stages from tight buds (0) to bloom (8). Each point represents the average and standard error of the damage score for a given structure or phenological stage reached ($n = 15$). Lines represent fitted curves by the Gompertz function

TABLE 2 Estimated BLT_{50}, GLT_{50}, and T_{max} values for *Vaccinium macrocarpon* terminal buds calculated from bud freeze damage and growth viability evaluations after controlled freezing tests

	BLT_{50} ± SE (°C)						
Sampling date	Bud axis	Bud scales	Flower primordia	Stem section	SAM	GLT_{50} ± SE (°C)	T_{max} ± SE (°C)
2018							
19 March	−29.0 ± 0.04	−30.7 ± 0.05	−36.3 ± 0.08	−37.2 ± 0.04	−40.8 ± 0.23	−31.8 ± 0.07	−33.0 ± 0.06
2 April	−28.0 ± 0.03	−30.5 ± 0.06	−35.8 ± 0.07	−37.1 ± 0.04	−38.3 ± 0.12	−26.6 ± 0.07	−28.9 ± 0.08
10 April	−34.8 ± 0.03	−35.1 ± 0.03	−37.1 ± 0.04	−36.8 ± 0.02	−38.4 ± 0.04	−31.7 ± 0.04	−33.0 ± 0.04
24 April	−28.3 ± 0.02	−30.3 ± 0.03	−27.2 ± 0.04	−32.1 ± 0.02	−33.0 ± 0.04	−25.7 ± 0.02	−26.7 ± 0.02
1 May	−12.4 ± 0.01	−10.7 ± 0.01	−13.2 ± 0.01	−13.7 ± 0.01	−13.7 ± 0.01	−11.9 ± 0.01	−12.3 ± 0.01
8 May	−10.9 ± 0.01	−10.5 ± 0.01	−11.6 ± 0.01	−17.2 ± 0.01	−11.9 ± 0.01	−12.6 ± 0.02	−13.3 ± 0.01
2019							
1 April	−32.1 ± 0.03	−36.5 ± 0.03	−31.5 ± 0.03	−32.3 ± 0.02	−33.7 ± 0.03	−30.6 ± 0.02	−31.3 ± 0.02
19 April	−25.9 ± 0.03	−26.8 ± 0.04	−24.4 ± 0.09	−27.6 ± 0.03	−28.5 ± 0.04	−24.8 ± 0.08	−27.1 ± 0.08
25 April	−19.2 ± 0.02	−20.2 ± 0.02	−21.5 ± 0.02	−25.7 ± 0.01	−21.8 ± 0.02	−22.4 ± 0.01	−22.9 ± 0.01
2 May	−18.8 ± 0.02	−19.0 ± 0.02	−22.2 ± 0.03	−23.2 ± 0.02	−21.8 ± 0.04	−23.5 ± 0.03	−24.0 ± 0.03
9 May	−19.4 ± 0.02	−17.5 ± 0.02	−20.8 ± 0.01	−22.4 ± 0.01	−20.8 ± 0.02	−16.9 ± 0.03	−17.5 ± 0.02

Note: The BLT_{50} is the temperature corresponding to 50% severity of browning and water soaking in each evaluated bud structure, based on a scale from 0 (no damage) to 3 (maximal damage). The GLT_{50} represents the temperature of 50% growth viability, as determined from the Gompertz function fitted to CFT data. T_{max} is the temperature of the maximal rate of growth viability loss. BLT_{50}, GLT_{50}, T_{max}, and standard error estimates were calculated as the mean from multiple runs ($n = 1000$) generated from a bootstrapping procedure.

TABLE 3 Estimated relative freezing damage values of *Vaccinium macrocarpon* bud structures at their corresponding GLT_{50} temperature

	Estimated relative freeze damage score at the GLT_{50} ± SE				
Sampling date	Bud axis	Bud scales	Flower primordia	Stem section	SAM
2018					
19 March	1.9 ± 0.006	1.6 ± 0.004	1.0 ± 0.009	0.6 ± 0.009	1.0 ± 0.008
2 April	1.2 ± 0.008	1.0 ± 0.007	0.3 ± 0.009	0.1 ± 0.005	0.4 ± 0.009
10 April	1.1 ± 0.004	1.3 ± 0.002	0.8 ± 0.006	0.1 ± 0.004	0.3 ± 0.007
24 April	0.9 ± 0.010	1.0 ± 0.005	1.3 ± 0.006	0.1 ± 0.003	0.2 ± 0.007
1 May	1.3 ± 0.007	2.5 ± 0.004	0.6 ± 0.010	0.2 ± 0.005	0.2 ± 0.005
8 May	2.2 ± 0.004	2.6 ± 0.004	1.8 ± 0.004	0.4 ± 0.004	1.7 ± 0.004
Average 2018	1.4 ± 0.007	1.7 ± 0.009	1.0 ± 0.007	0.2 ± 0.003	0.6 ± 0.008
2019					
1 April	1.2 ± 0.006	0.9 ± 0.004	1.3 ± 0.008	0.9 ± 0.007	0.7 ± 0.009
19 April	1.1 ± 0.009	1.1 ± 0.009	1.3 ± 0.016	0.6 ± 0.010	0.4 ± 0.009
25 April	2.0 ± 0.003	1.9 ± 0.003	1.6 ± 0.003	0.3 ± 0.006	1.6 ± 0.006
2 May	2.4 ± 0.002	2.3 ± 0.002	2.2 ± 0.003	1.7 ± 0.004	2.0 ± 0.003
9 May	0.8 ± 0.009	1.4 ± 0.006	0.2 ± 0.007	0.0 ± 0.000	0.2 ± 0.005
Average 2019	1.5 ± 0.009	1.5 ± 0.007	1.3 ± 0.010	0.7 ± 0.009	1.0 ± 0.010
Average 2018–2019	1.4 ± 0.005	1.6 ± 0.006	1.1 ± 0.006	0.4 ± 0.005	0.8 ± 0.007

Note: The GLT_{50} represents the temperature of 50% growth viability, as determined from the Gompertz function fitted to CFT data. Freeze damage values correspond to the severity of browning and water soaking in the bud structure after CFT, based on a scale from 0 (no damage) to 3 (maximal damage). Estimates of relative freezing damage values at the GLT_{50} temperature were calculated using the Gompertz fitted curve for each bud structure. Relative freezing damage, GLT_{50}, and standard error estimates were calculated as the mean from multiple runs ($n = 1000$) generated from a bootstrapping procedure.

logistic regression with a quasibinomial distribution (Figure 6). In the model, the seasonal factor Early Spring (dates before May 1, 2018 and April 25, 2019) and Late Spring (dates after May 1, 2018, and April 25, 2019) were not significant. The Hosmer-Lemeshow goodness of fit test for logistic regression results was $\chi^2 = 1.8015$, with eight degrees of freedom, and a p-value = 0.9865 indicating no evidence of poor fit.

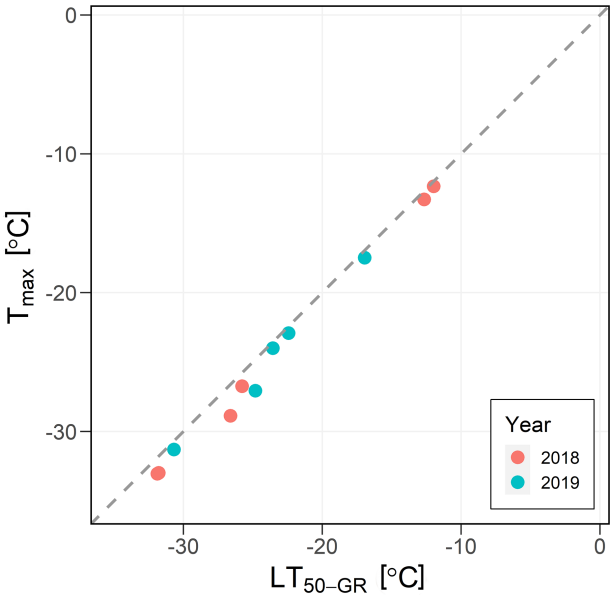

FIGURE 5 Plot of *Vaccinium macrocarpon* terminal bud GLT_{50} and T_{max} values for all sampling dates in spring 2018 and 2019. The GLT_{50} is the temperature of 50% growth viability and T_{max} is the temperature of the maximal rate of growth viability loss. The dashed line illustrates the hypothetical case if T_{max} equaled GLT_{50}

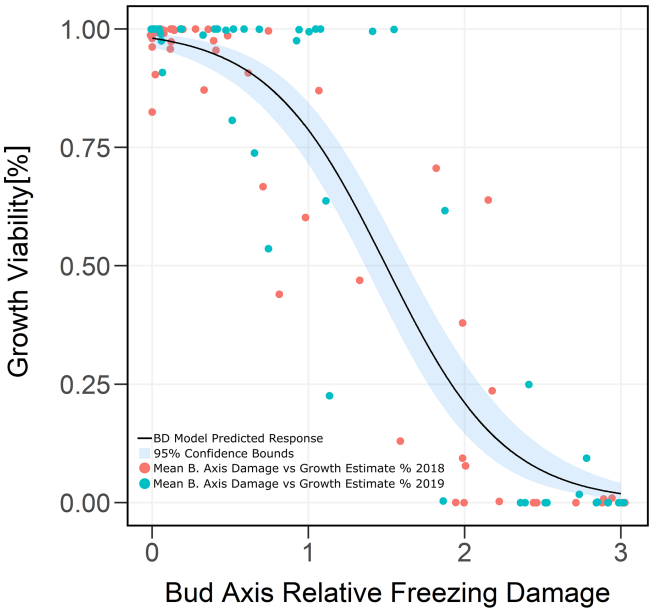

FIGURE 6 Percentage of growth viability in relation to the relative mean freeze damage of the bud axis during the springs of 2018 and 2019. Each point represents the mean damage score for the bud axis ($n = 15$) at one of the controlled freezing test temperatures and the corresponding mean growth viability percentage estimate. The black curve is the growth viability response to bud axis damage predicted by the constructed bud damage model and the blue area represents the 95% confidence bounds

3.5 | Cold hardiness model (CH model)

The explanatory model for GLT_{50} temperatures in relation to environmental parameters was a linear regression with a normal distribution (Figure 3). The selected CH model had two parameters: σ_{T10} for daily minimum and σ_{T10} for daily maximum temperatures. Estimates for the intercept were −31.327, σ_{T10} for daily minimum was 0.264, and σ_{T10} for daily maximum was 0.144. This model had a *p*-value of 0.0005, and an adjusted-$R^2 = 0.8093$. The dominance analysis for the two variables in the CH model resulted in a 51.1% and 33.7% relative importance for σ_{T10} for daily maximum and σ_{T10} for daily minimum temperature, respectively.

4 | DISCUSSION

The objectives of this study were to investigate the relationship between freeze damage in terminal buds during ecodormancy and their viability during the subsequent growing season, and to identify the bud structure that best represents this relationship. We estimated the temperature corresponding to 50% severity of browning and water soaking in each evaluated bud structure, referred to as the Browning LT_{50} (BLT_{50}). Similarly, we determined the temperature at which growth viability was impaired by 50%, referred to as the Growth LT_{50} (GLT_{50}). Through the development of a bud damage model, we determined that the bud axis was the bud structure whose relative freeze damage correlated best to patterns of growth viability reduction. Finally, we developed a model that utilizes the temperature parameters σ_{T10} for daily maximum and σ_{T10} for daily minimum temperatures to explain changes in the GLT_{50} during ecodormancy.

A negative correlation between freeze damage in bud structures and growth viability of the upright was observed across the entire sampling period. All damage and growth viability curves were sigmoidal, but in opposite directions (Figure 4), which is a commonly described freezing damage response in plant tissues (Zhu & Liu, 1987). In the growth viability data, the asymmetrical nature of the sigmoidal relationship was confirmed by the differences between T_{max} and GLT_{50} values, where T_{max} was consistently detected at lower temperatures (Workmaster & Palta, 2006; Figure 5). This difference was greater in Early Spring than in Late Spring, meaning that the maximum rate of damage results at lower percentages of growth viability in early versus late spring. In both years, with spring deacclimation, GLT_{50} values moved to warmer temperatures (Figure 3) with a higher rate of deacclimation in late April to early May, as described by others for *V. macrocarpon* (Abdallah & Palta, 1989; Villouta et al., 2020; Workmaster & Palta, 2006).

4.1 | Bud structure selection for BD model construction

Within a plant, freezing stress resistance levels can vary significantly across tissues and organs (Glerum, 1985; Sakai & Larcher, 1987). In our study, the severity of freezing damage fluctuated across the five

identified structures of the bud over the entire sampling period (Table 2). In comparing the bud structure freezing damage severity at the GLT_{50}, bud scales and bud axis had consistently the highest damage scores, while the stem section and SAM had the lowest damage scores (Table 3). The variability in damage among bud structures highlights the importance of identifying the most relevant tissues and/or organs for extrapolation to whole shoot viability (Embree & McRae, 1991). Taking this into consideration, we created an explanatory bud damage model (BD model) to describe *V. macrocarpon* upright growth viability using a single bud structure.

The selection of the most appropriate bud structure to develop the BD model in *V. macrocarpon* was based on two criteria: level of correlation to growth viability and observer ability to accurately evaluate the damage. Each of the five bud structures had a high correlation value between freezing damage and the percentage of growth viability, ranging from −0.87 for the stem section and SAM to −0.92 for the bud axis. Despite the high correlations for all the evaluated structures, there was a wide range of damage scores for each structure at their respective GLT_{50} temperature. For example, at 50% growth viability, the bud scales and SAM had average damage scores of 1.6 and 0.8, respectively (Table 3). In addition, across the sampling dates, the differences in °C between the BLT_{50} values for each bud structure and the GLT_{50} (Figure 7) ranged from +2.4°C for the bud axis to −11.7°C for the SAM. For example, by early April 2018, the GLT_{50} was −26.6°C; however, the bud axis and SAM BLT_{50} values were −28.0 and −38.3°C, respectively, nearly a 10°C difference (Table 2). As a result, we conclude that the correlation values are not as informative as the correspondence between BLT_{50} and GLT_{50} in determining which bud structure's freezing stress response is the most relevant to subsequent bud growth viability.

The observer's ability to accurately assess plant tissue freezing stress damage is the basis of visual evaluation. However, the methodology of tissue damage scoring is inherently subjective, at least in part (Ritchie, 1991). In our methodology, bud structure definition and the levels of damage severity were previously determined (Villouta et al., 2020). Yet, there were still challenges when scoring damage in each structure. In the case of flower primordia, longitudinal dissection of buds does not expose all of the primordia due to their whorled pattern (Bolivar-Medina et al., 2018), resulting in a potentially inaccurate damage scoring. The stem section and SAM had low incidences of browning damage at the respective GLT_{50} temperatures (Table 3), which hindered the correlation between damage and growth viability. The low incidence of damage in the SAM has been interpreted as the result of its adaptation to dehydration as a mechanism of cold tolerance (Villouta et al., 2020). Damage in the SAM was also difficult to score due to its small size, which resulted in the most variability in damage scores at a given CFT temperature (Table S1). In the case of bud scales, their complex shape challenges the scoring process compared to other structures, which also resulted in a high dispersion of observed levels of damage (Table S1). From all the evaluated structures, the bud axis was the easiest to score, due to its well defined and relatively larger area (Figure 1). In addition, the bud axis incurs damage at relatively warmer temperatures than the SAM, flower primordia, and stem section (Abdallah & Palta, 1989; Villouta et al., 2020; Workmaster & Palta, 2006). Finally, the bud axis BLT_{50} values were closer to the GLT_{50} values than for any of the other structures (Figure 7). Based on all these observations, the bud axis was the best candidate for modeling purposes due to both the correlation between its BLT_{50} and the corresponding GLT_{50} and the relative ease of the observer's ability to evaluate the damage accurately.

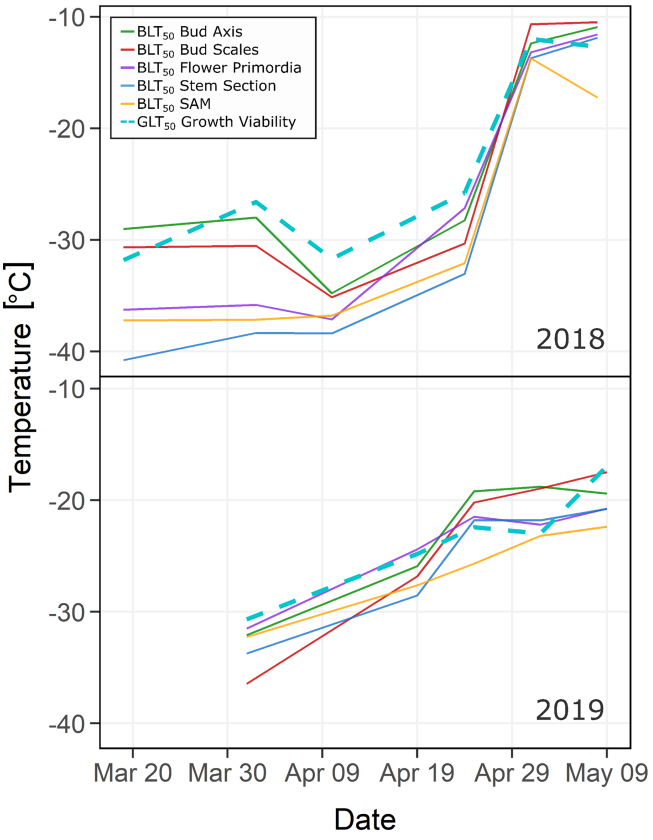

FIGURE 7 GLT_{50} and BLT_{50} by bud structure for 2018 and 2019 sampling dates. The BLT_{50} is the temperature corresponding to 50% severity of browning and water soaking in each evaluated bud structure, based on a scale from 0 (no damage) to 3 (maximal damage). The GLT_{50} represents the temperature of 50% growth viability. T_{max} represents the temperature of the maximal rate of growth viability loss. GLT_{50}, BLT_{50}, T_{max}, and standard error estimates were calculated as the mean from multiple runs ($n = 1000$) generated from a bootstrapping procedure

The resulting BD explanatory model illustrates the negative relationship between the bud axis damage severity and the percentage of bud growth viability after exposure to freezing stress (Figure 6). Previous work has surmised that the bud axis, as a gateway for water mobilization to the bud, experiences faster dehydration than other parts of the bud when exposed to freezing temperatures, making it more vulnerable to injury (Quamme, 1995). This role of the bud axis was also used to explain how the health of this bud structure relates to the cold hardiness and survivability of the entire subsequent shoot (Workmaster & Palta, 2006), and to hypothesize the coordinated movement of water within and between bud structures in the freezing stress survival strategy of *V. macrocarpon* buds (Villouta et al., 2020).

The BD model depicts a sigmoidal curve, where there is a threshold of damage that once surpassed, growth viability decreases rapidly. The level of tissue browning where this threshold was observed in the BD explanatory model occurred between ratings 1 and 2, which is also the range with the highest variability in the percentage of growth viability in response to freezing stress (Figure 6). A source of this variability could come from the BLT_{50} seasonal shift, moving from underestimation of the GLT_{50} in Early Spring to a partial overestimation in Late Spring (Figure 7). The browning freeze damage response is also modulated by an increase in the polyphenol oxidase activity at the end of the rest season (Zahra et al., 2009). The interaction between these two factors, cold hardiness and damage expression, could lead to imprecise estimations of cold hardiness and chronic damage. Another component contributing to variability in the GLT_{50} at this damage threshold is the risk of the subjectivity of visual evaluations (Luoranen et al., 2004; Odlum & Blake, 1996; Ritchie, 1991), regardless of the use of standardization of tissue damage severities. Future studies targeting the development of a predictive model would need to address these contributing factors to variability, as well as the number of data points and sampling locations, and an eventual model validation of post-freezing outcomes under field conditions.

4.2 | Selection of environmental factors and CH model construction

Our second objective was to determine which environmental factors best explain the variations in cold hardiness during ecodormancy. The resulting cold hardiness (CH) model described the effect of temperature across the seasonal changes in the GLT_{50} (adjusted-$R^2 = 0.81$) during the two evaluated years (Figure 3). From all the variables considered during the model construction, the backward stepwise procedure selected the temperature indices σ_{T10} using daily maximum temperatures and σ_{T10} using daily minimum temperature as the most significant set of variables to explain the seasonal GLT_{50} changes. Two important components of plant temperature experience are reflected in the selection of these variables for the explanation of spring bud cold hardiness changes: first, the temperature range to which the vines are exposed, and second, the cumulative effect of this temperature experience for a specific time bracket (the preceding 10 days).

The daily maximum and minimum temperature components in our model represent the range of temperature fluctuation experienced by the vines. Temperature fluctuations have been described as more impactful to cold hardiness changes, in comparison to constant temperatures (Hamilton, 1972). Part of this influence is due to the antagonist processes of deacclimation and reacclimation, where deacclimation is driven by the daily maximum temperatures but modulated by the daily minimum temperatures (Kalberer et al., 2006). Studies of a group of *Vaccinium* species reported that the plants' cold hardiness changes could be the result of daily deacclimation and reacclimation processes driven by the exposure to the daily maximum and minimum temperatures (Arora et al., 2004; Rowland et al., 2005). In the specific case of *V. macrocarpon*, cold hardiness changes appear to be driven more by the σ_{T10} for daily maximum than the σ_{T10} for daily minimum temperatures. As seen in the dominance analysis for the model, these variables had 51.1% and 33.7% relative importance, respectively. σ_{T10} for daily maximum temperatures would account for the deacclimation process, which has been described to occur at faster rates than reacclimation (Arora & Taulavuori, 2016; Howell & Weiser, 1970).

The temperature indices used in the CH model describe how cold hardiness is greatly influenced by the most recent environmental conditions experienced by the plants (Gay & Eagles, 1991; Kalberer et al., 2006). To determine the most influential range of days for *V. macrocarpon*, periods of 7, 10, 12, and 14 days were compared for σ_T calculations. The variable σ_{T10} was found to best represent this lag between the exposure to temperatures (daily maximum and minimum) and the current state of the plant deacclimation response for *V. macrocarpon*. This lag period has been reported to differ across species, such as *Vaccinium* sp., *Rhododendron* sp., *Hydrangea* sp., and wild grapes (Arora et al., 2004; Liu et al., 2017; Londo & Kovaleski, 2017; Pagter et al., 2011; Rowland et al., 2005). Multiple factors contribute to this diversity in response, such as the region of species origin, genotype, dormancy stage, and environmental conditions (Arora & Taulavuori, 2016). The relatively shorter period of 10 days for *V. macrocarpon*, a woody trailing evergreen vine, in comparison to the 14 days reported for the interspecific hybrids of evergreen rhododendron (Liu et al., 2017), could be an evolutionary difference in this trait, driven by their different growth habits and exposures to air temperature variations. *V. macrocarpon* grows in low lying areas and is mostly under snow cover during the dormant period (Eck, 1990). In contrast, *Rhododendron* spp. are shrubs with heights ranging between 0.5 and 4.5 m (Chamberlain & Rae, 1990). The capacity of temperate and boreal species to incorporate a moving range of temperature experiences into their physiological responses enables the avoidance or tempering of deacclimation during warm spells in late winter and minimizes the impact of exposure to spring freezing events and the loss of critical time for growth (Vyse et al., 2019).

5 | CONCLUSION

In this study, we established that freezing damage to the bud axis is the most relevant indicator for subsequent upright growth and development, which is a departure from the traditional damage evaluation technique that focuses solely on the perceived health of the flower primordia. The high correspondence between freezing damage and growth viability, coupled with the ease of evaluation of this structure, makes the bud axis an ideal candidate for cold hardiness phenotype screening in breeding selection. The quest to relate temperature experience to changes in spring bud cold hardiness has to date mostly focused on the development of models based on the accumulation of thermal time (e.g., growing degree days). The cold hardiness model developed in this study accounts for the effect of temperature fluctuations in spring on the deacclimation and reacclimation dynamics of

buds within a continually rolling timeframe (σ_{T10}). Our cold hardiness model offers promising results, which after further and intensive testing, could provide a foundation for the development of a decision-making tool for farmers that will be accomplished upon completion of field validation trials.

ACKNOWLEDGMENTS

We would like to thank Bill Wolfe from Wisconsin River Cranberry Co. for supporting our research by allowing access to his farm and to Smith Sinclair for his assistance in data collection.

AUTHOR CONTRIBUTIONS

Study conception and design were completed by Amaya Atucha, Beth Ann Workmaster, and Camilo Villouta Methodology implementation was performed by Amaya Atucha, Beth Ann Workmaster, and Camilo Villouta. Experiment execution and data collection were carried out by Camilo Villouta. Data analysis/interpretation and manuscript writing were done by Amaya Atucha, Beth Ann Workmaster, and Camilo Villouta.

DATA AVAILABILITY STATEMENT

The data that support the findings of this study are available from the corresponding author upon reasonable request.

ORCID

Camilo Villouta https://orcid.org/0000-0002-1762-6013

REFERENCES

Abdallah, A.Y. & Palta, J.P. (1989) Changes in the freezing stress resistance of the cranberry leaf, flower bud, and fruit during growth and development. *Acta Horticulturae*, 241, 273–276.

Arora, R. & Taulavuori, K. (2016) Increased risk of freeze damage in woody perennials VIS-À-VIS climate change: importance of deacclimation and dormancy response. *Frontiers in Environmental Science*, 4, 44.

Arora, R., Rowland, L.J., Ogden, E.L., Dhanaraj, A.L., Marian, C.O., Ehlenfeldt, M.K. et al. (2004) Dehardening kinetics, bud development, and dehydrin metabolism in blueberry cultivars during deacclimation at constant, warm temperatures. *Journal of the American Society for Horticultural Science*, 129, 667–674.

Augspurger, C.K. (2013) Reconstructing patterns of temperature, phenology, and frost damage over 124 years: spring damage risk is increasing. *Ecology*, 94, 41–50.

Bolivar-Medina, J.L., Zalapa, J., Atucha, A. & Patterson, S.E. (2018) Relationship of alternate bearing and apical bud development in cranberry (*Vaccinium macrocarpon* Ait.). *Botany*, 97(2), 101–111.

Burr, K.E., Tinus, R.W., Wallner, S.J. & King, R.M. (1990) Comparison of three cold hardiness tests for conifer seedlings. *Tree Physiology*, 6, 351–369.

Chamberlain, D.F. & Rae, S.J. (1990) A revision of rhododendron. IV subgenus Tsutsusi. *Edinburgh Journal of Botany*, 47(2), 89–200.

DeMoranville, C. & Demoranville, I. (1997) Cold tolerance of cranberry flower buds differs by cultivar and developmental stage. *HortScience*, 32, 538–538.

DeMoranville, C.J., Davenport, J.R., Patten, K., Roper, T.R., Strik, B.C., Vorsa, N. et al. (1996) Fruit mass development in three cranberry cultivars and five production regions. *Journal of the American Society for Horticultural Science*, 121(4), 680–685.

Eck, P. (1990) *The American cranberry*. New Brunswick, NJ: Rutgers University Press.

Embree, C.G. & McRae, K.B. (1991) An exploratory study of reciprocal apple rootstock and scion hardiness with two methods of assessment. *HortScience*, 26, 1523–1525.

Gay, A.P. & Eagles, C.F. (1991) Quantitative analysis of cold hardening and dehardening in Lolium. *Annals of Botany*, 67, 339–345.

George, M.F., Burke, M.J., Pellett, H.M. & Johnson, A.G. (1974) Low temperature exotherms and woody plant distribution. *HortScience*, 9, 519–522.

Glerum, C. (1985) Frost hardiness of conifer seedlings: principles and applications. In: Duryea, M.L. (Ed.) *Evaluating seedling quality: principles, procedures, and predictive abilities of major tests, proceedings of a workshop held October 16–18, 1984*. Corvallis, OR: Forest Research Laboratory, Oregon State University, pp. 107–123.

Gordon-Kamm, W.J. & Steponkus, P.L. (1984) Lamellar-to-hexagonalII phase transitions in the plasma membrane of isolated protoplasts after freeze-induced dehydration. *Proceedings of the National Academy of Sciences*, 81, 6373–6377.

Hamilton, D.F. (1972) Factors influencing dehardening and rehardening of *Forsythia x intermedia* stems. *Journal of the American Society for Horticultural Science*, 98(1973), 221–223.

Howell, G.S. & Weiser, C.J. (1970) The environmental control of cold acclimation in apple. *Plant Physiology*, 45, 390–394.

Inouye, D.W. (2000) The ecological and evolutionary significance of frost in the context of climate change. *Ecology Letters*, 3, 457–463.

Kalberer, S.R., Wisniewski, M. & Arora, R. (2006) Deacclimation and reacclimation of cold-hardy plants: current understanding and emerging concepts. *Plant Science*, 171, 3–16.

Larsen, H.J. (2009) Evaluating tree fruit bud & fruit damage from cold. Colorado State University Extension. Available from: https://extension.colostate.edu/topic-areas/yard-garden/evaluating-tree-fruit-bud-fruit-damage-from-cold-7-426/ [Accessed 10th October 2020].

Levitt, J. (1980) Responses of plants to environmental stress. In: *Chilling, freezing, and high temperature stresses*, Vol. 1, 2nd edition. London, New York, NY: Academic Press.

Lim, C.C., Arora, R. & Townsend, E.C. (1998) Comparing Gompertz and Richards functions to estimate freezing injury in rhododendron using electrolyte leakage. *Journal of the American Society for Horticultural Science*, 123, 246–252.

Liu, B., Zhou, H., Cao, S., Xia, Y.P. & Arora, R. (2017) Comparative physiology of natural deacclimation in ten azalea cultivars. *HortScience*, 52, 1451–1457.

Londo, J.P. & Kovaleski, A.P. (2017) Characterization of wild North American grapevine cold hardiness using differential thermal analysis. *American Journal of Enology and Viticulture*, 68, 203–212.

Luoranen, J., Repo, T. & Lappi, J. (2004) Assessment of the frost hardiness of shoots of silver birch (*Betula pendula*) seedlings with and without controlled exposure to freezing. *Canadian Journal of Forest Research*, 34, 1108–1118.

Moyer, M., Mills, L., Hoheisel, G., Keller, M. (2011) Assessing and managing cold damage in Washington vineyards. EM043e. Washington State UniversityExtension Publishing. Available from: http://pubs.cahnrs.wsu.edu/publications/wp-content/uploads/sites/2/publications/em042e.pdf [Accessed January 11, 2021]

Odlum, K.D. & Blake, T.J. (1996) A comparison of analytical approaches for assessing freezing damage in black spruce using electrolyte leakage methods. *Canadian Journal of Botany*, 74, 952–958.

Olszewski, F., Jeranyama, P., Kennedy, C.D. & DeMoranville, C.J. (2017) Automated cycled sprinkler irrigation for spring frost protection of cranberries. *Agricultural Water Management*, 189, 19–26.

Pagter, M., Hausman, J.F. & Arora, R. (2011) Deacclimation kinetics and carbohydrate changes in stem tissues of hydrangea in response to an experimental warm spell. *Plant Science*, 180, 140–148.

Palta, J.P., Levitt, J. & Stadelmann, E.J. (1977a) Freezing injury in onion bulb cells: II. Post-thawing injury or recovery. *Plant physiology*, 60, 398–401.

Palta, J.P., Levitt, J. & Stadelmann, E.J. (1977b) Freezing injury in onion bulb cells: I. evaluation of the conductivity method and analysis of ion and sugar efflux from injured cells. *Plant Physiology*, 60, 393–397.

Parker, J. (1963) Cold resistance in woody plants. *The Botanical Review*, 29, 123–201.

Quamme, H.A. (1995) Deep supercooling in buds of woody plants. In: Lee, R.E., Warren, G.J. & Gusta, L.V. (Eds.) *Biological ice nucleation and its applications*. Minneapolis, MN: APS Press, pp. 183–199.

Ritchie, G.A. (1991) Measuring cold hardiness. In: Lassoie, J.P. & Hinckley, T.M. (Eds.) *Techniques and approaches in forest tree ecophysiology*. Boca Raton, FL: CRC Press, pp. 557–582.

Rodrigo, J. (2000) Spring frosts in deciduous fruit trees – morphological damage and flower hardiness. *Scientia Horticulturae*, 85, 155–173.

Rowland, L.J., Ogden, E.L., Ehlenfeldt, M.K. & Vinyard, B. (2005) Cold hardiness, deacclimation kinetics, and bud development among 12 diverse blueberry genotypes under field conditions. *Journal of the American Society for Horticultural Science*, 130, 508–514.

Sakai, A. & Larcher, W. (1987) *Frost survival of plants: responses and adaptation to freezing stress*, Vol. 62. Berlin: Springer-Verlag.

Salazar-Gutiérrez, M.R., Chaves, B. & Hoogenboom, G. (2016) Freezing tolerance of apple flower buds. *Scientia Horticulturae*, 198, 344–351.

Steponkus, P.L. (1984) Role of the plasma membrane in freezing injury and cold acclimation. *Annual Review of Plant Physiology*, 35, 543–584.

Stergios, B.G. & Howell, G.S. (1973) Evaluation of viability tests for cold stressed plants. *Journal of the American Society for Horticultural Science*, 98(4), 325–330.

Takahashi, D., Uemura, M. & Kawamura, Y. (2018) Freezing tolerance of plant cells: from the aspect of plasma membrane and microdomain. In: Iwaya-Inoue, M., Sakurai, M. & Uemura, M. (Eds.) *Survival strategies in extreme cold and desiccation*. Advances in experimental medicine and biology, Vol. 1081. Singapore: Springer, pp. 61–79.

Vasseur, D.A., DeLong, J.P., Gilbert, B., Greig, H.S., Harley, C.D.G., McCann, K.S. et al. (2014) Increased temperature variation poses a greater risk to species than climate warming. *Proceedings of the Royal Society B*, 281, 20132612.

Villouta, C., Workmaster, B.A., Bolivar-Medina, J., Sinclair, S. & Atucha, A. (2020) Freezing stress survival mechanisms in *Vaccinium macrocarpon* Ait. terminal buds. *Tree Physiology*, 40, 841–855.

Vyse, K., Pagter, M., Zuther, E. & Hincha, D.K. (2019) Deacclimation after cold acclimation—a crucial, but widely neglected part of plant winter survival. *Journal of Experimental Botany*, 70, 4595–4604.

Warrington, I.J. & Rook, D.A. (1980) Evaluation of techniques used in determining frost tolerance of forest planting stock: a review. *New Zealand Journal of Forest Science*, 10, 116–132.

Webb, M.S., Uemura, M. & Steponkus, P.L. (1994) A comparison of freezing injury in oat and rye: two cereals at the extremes of freezing tolerance. *Plant Physiology*, 104, 467–478.

Williams, C.M., Henry, H.A.L. & Sinclair, B.J. (2015) Cold truths: how winter drives responses of terrestrial organisms to climate change. *Biological Reviews*, 90, 214–235.

Workmaster, B.A.A. & Palta, J.P. (2006) Shifts in bud and leaf hardiness during spring growth and development of the cranberry upright: regrowth potential as an indicator of hardiness. *Journal of the American Society for Horticultural Science*, 131, 327–337.

Workmaster, B.A.A., Palta, J.P. & Roper, T.R. (1997) Terminology for cranberry bud development and growth. *Cranberries*, 61, 11–14.

Zahra, P., Majid, R. & Amin, B. (2009) Seasonal changes of peroxidase, polyphenol oxidase enzyme activity and phenol content during and after rest in pistachio (*Pistacia vera* L.) flower buds. *World Applied Sciences Journal*, 6, 1193–1199.

Zhu, G.H. & Liu, Z.Q. (1987) Determination of median lethal temperature using logistic function. In: Li, P.H. (Ed.) *Plant cold hardiness*. New York, NY: Alan R. Liss, pp. 291–298.

SUPPORTING INFORMATION

Additional supporting information may be found online in the Supporting Information section at the end of this article.

How to cite this article: Villouta, C., Workmaster, B.A. and Atucha, A. (2021) Freezing stress damage and growth viability in *Vaccinium macrocarpon* Ait. bud structures. *Physiologia Plantarum*, 172(4), 2238–2250. Available from: https://doi.org/10.1111/ppl.13457